# The substitutions G245C and G245D in the Zn$^{2+}$-binding pocket of the p53 protein result in differences of conformational flexibility of the DNA-binding domain

S.S. Pintus , N.V. Ivanisenko , P.S. Demenkov , T.V. Ivanisenko , S. Ramachandran , N.A. Kolchanov & V.A. Ivanisenko

Taylor & Francis
Taylor & Francis Group

# The substitutions G245C and G245D in the Zn$^{2+}$-binding pocket of the p53 protein result in differences of conformational flexibility of the DNA-binding domain

S.S. Pintus[a]*, N.V. Ivanisenko[a], P.S. Demenkov[a], T.V. Ivanisenko[a], S. Ramachandran[b], N.A. Kolchanov[a] and V.A. Ivanisenko[a]

[a]*Laboratory of Computational Proteomics, Institute of Cytology and Genetics SB RAS, Lavrentyev av. 10, Novosibirsk, 630090, Russia;* [b]*G.N. Ramachandran Knowledge Centre for Genome Informatics, Institute of Genomics and Integrative Biology (CSIR), Mall Road, Delhi 110 007, India*

Transcription activation of the proapoptotic target genes is a means by which the p53 protein implements its function of tumor suppression. Zn$^{2+}$ is a known regulator of p53 binding to the target genes. We have previously obtained an evidence that amino acid substitutions in the p53 Zn$^{2+}$-binding pocket can presumably exert an influence on Zn$^{2+}$ position in the Zn$^{2+}$-p53 complex and thereby affect p53 binding to DNA. With these background considerations, our aim was to estimate the effect of the putative changes in the Zn$^{2+}$ position in its binding pocket due to the G245C and G245D substitutions on the conformation of the p53 DNA-binding motif. Statistical analysis of the molecular dynamics (MD) trajectories of the mutant p53-Zn$^{2+}$ complexes was used to detect significant deviations in conformation of the mutant p53 forms. MD simulations demonstrated that (1) the two substitutions in the Zn$^{2+}$-binding pocket caused changes in the conformation of the p53 DNA-binding motif, as compared with the wild-type (WT) p53; (2) binding of Zn$^{2+}$ to the p53 mutant forms reduced the effect of the substitutions on conformational change; and (3) Zn$^{2+}$ binding in the normal position compensated the effect of the mutations on the conformation in comparison to the altered Zn$^{2+}$ position.

**Keywords:** p53 protein; molecular dynamics; conformational flexibility; DNA binding domain (DBD); binding site

## Introduction

The major functions of the p53 protein include the prevention of the division of cells with damaged DNA sites and involvement in the formation of embryonic organs in most vertebrates (Amariglio et al., 1997; Prochazkova et al., 2004). The p53 protein arrests the cell cycle at one of the control points or causes cell apoptosis when DNA is damaged. In such a case, p53 can act both as a transcription factor and an activator of the products of the other genes (Levine, 1997). The tumor suppression functions of p53 include also its direct participation in DNA excision repair (Donehower, 1997).

The p53 protein requires Zn$^{2+}$ to provide the association of p53 with the target genes (Pavletich, Chambers, & Pabo, 1993). Experiments have demonstrated that Zn$^{2+}$ loss rendered p53 incapable of binding to DNA (Butler & Loh, 2003). It is known that removal of Zn$^{2+}$ reduced the specificity of the p53 binding to DNA (Méplan, Richard, & Hainaut, 2000a; Rainwater, Parks,

Anderson, Tegtmeyer, & Mann, 1995). It is known that certain mutations that made p53 incapable of binding to Zn$^{2+}$ resulted in loss of p53 activity (Méplan, Richard, & Hainaut, 2000b). It has been observed also that Zn$^{2+}$ binding modulated the conformation of the DNA-binding domain (DBD) (Hainaut & Mann, 2001; Verhaegh, Parat, Richard, & Hainaut, 1998).

The data regarding the influence of mutations on the structure and function of p53 are abundant. Thus, it has been shown that mutations that influenced Zn$^{2+}$ binding exerted also an influence on p53 function. Certain mutations in the region of the Zn$^{2+}$-binding site made p53 partially or completely incapable of Zn$^{2+}$ binding, thereby resulting in the inactive conformation of the mutant p53 form (Butler & Loh, 2003). It is also noteworthy that mutations in the Zn$^{2+}$-binding pocket are associated with inferior prognosis for cancers (Alsner et al., 2008; Olivier et al., 2006; van Slooten et al., 1999). Particularly, germline substitutions G245C and

G245D, which reside in this pocket, are associated with the Li-Fraumeni syndrome, which is the one of the well-studied family cancers (Malkin et al., 1990).

The molecular dynamics (MD) simulations have demonstrated the effect of mutations and $Zn^{2+}$ binding in p53 DBD on p53 structure. Evidence was obtained indicating that mutations in the DBD structural elements result in changes of their conformational flexibility (Merabet et al., 2010). Furthermore, results of MD simulations have shown that $Zn^{2+}$ binding in the p53 DBD had an impact on its stability and its binding to DNA (Duan & Nilsson, 2006). Another relevant finding was that a number of mutations in the region of the $Zn^{2+}$ binding caused loss of the p53 stability (Lu, Tan, & Luo, 2007).

We have previously suggested that amino acid substitutions in the $Zn^{2+}$ structural pocket can have an influence on $Zn^{2+}$ position in the $Zn^{2+}$-DBD complex and, in so doing, influence p53-DNA binding. We have predicted an alternative potential $Zn^{2+}$-binding site in the mutant DBD form (Ivanisenko, Pintus, Grigorovich, & Kolchanov, 2005) and analyzed energies of $Zn^{2+}$ binding in this site (Pintus, Fomin, Ivanisenko, & Kolchanov, 2006; Pintus, Fomin, Oshurkov, & Ivanisenko, 2007).

The aim of this study was to estimate the putative effect of the position of $Zn^{2+}$ in its binding pocket on the conformation of the DNA-binding motif of p53 mutants. Thus, we compared effects of $Zn^{2+}$ binding to predicted and normal sites on p53 DBD conformation.

MD simulations were used to analyze the $Zn^{2+}$-DBD complexes. To detect significant deviations of the conformation of the mutant p53 forms from wild-type (WT), a statistical approach was applied. With this approach, the MD trajectories of WT and mutant p53 DBD forms were compared. Here, we showed that amino acid substitutions in the $Zn^{2+}$-binding pocket resulted in conformational changes in the DNA-binding motif of the p53 protein compared with WT. We showed also that the position of $Zn^{2+}$ in its binding pocket had an influence on the conformation of the mutant form, partly compensating the mutation effect on the p53 DBD conformation more in the normal than in the modified position.

## Materials and methods

### Prediction of $Zn^{2+}$ position in the tertiary structures of p53 mutants

$Zn^{2+}$-binding sites were searched in the human mutant p53 DBD structures using the web server PDBSiteScan (Ivanisenko, Pintus, Grigorovich, & Kolchanov, 2004). The search relied on the superimposition of functional site templates taken from the PDBSite database with the p53 tertiary structure (Lu et al., 2007).

To obtain tertiary structures for the p53 DBD mutants, homology-based predictions were made using the SWISS-MODEL server (Schwede, Kopp, Guex, & Peitsch, 2003). An appropriate amino acid substitution was introduced into an amino acid sequence of the human p53 DBD retrieved from the SWISS-PROT database (ID P53_HUMAN); then, a tertiary structure was derived from the resulting sequence using homology-based prediction; the X-ray structure of the human p53 DBD (PDB ID 1GZH) served as a template. Zn-binding sites were searched with the PDBSiteScan tool in the resulting tertiary structures. The PDBSiteScan web server provided both superimposition of site templates and p53 DBD structure and positioning of $Zn^{2+}$ in binding pocket.

In this way, the conformation of the residues of the found potential site and the coordinates of its ligand taken from the site templates were roughly defined. These were more accurately defined using MD as described below.

### Molecular dynamics

GROMACS molecular dynamics package v. 4.5.3 (Hess, Kutzner, van der Spoel, & Lindahl, 2008) was used to perform 1 ns (nanosecond) MD simulation applying the OPLS force field (Jorgensen & Tirado-Rives, 1988; Jorgensen, Maxwell, & Tirado-Rives, 1996). The explicit water model TIP4P (Jorgensen, Chandrasekhar, Madura, Impey, & Klein, 1983) was used for this study. The simulation box size was $75 A \times 75 A \times 75 A$. Appropriate amounts of $Cl^-$ anions were added to maintain electroneutrality. The simulation system was set up as an NPT ensemble. Periodic boundary conditions were used and the electrostatic interactions (long range) were evaluated by using the Ewald summation (Ewald, 1921) as implemented in the Particle Mesh Ewald (PME) method (Esmann et al., 1995) with a real space cut-off of 14 Å, 1.2 Å spacing of the Fourier grid, a sixth-order β-spline, and direct sum tolerance of $10-6$. A 14 Å cut-off was used in the evaluation of van der Waals interactions (short range). A time step of 2 fs was used.

To model $Zn^{2+}$ binding to residues of the $Zn^{2+}$-binding site, the bonded approach was adopted. It is implemented in the GROMACS program with the use of the covalent bond potential. The force constant (40 kcal $Å^{-1} = 1673.6$ kJ nm$^{-1}$) and equilibrium Zn–N bond length (2.05 Å = 0.205 nm) values were taken from quantum mechanics calculations (Coi, Tonelli, Ganadu, & Bianucci, 2006). The equilibrium Zn–S bond value was set equal to Zn–N bond (0.205 nm). The potentials of bond and dihedral angle potentials were omitted.

The starting structures of the $Zn^{2+}$–DBD complex were first subjected to unconstrained minimization with 500 steps in the presence of TIP4P water molecules (the atom position restraining force was 10,000 kJ mol$^{-1}$ nm$^{-2}$). This was followed by energy minimization with 2500 steps applied on TIP4P water molecules, while position restraints (the restraining force was 10,000 kJ mol$^{-1}$

$nm^{-2}$) were applied on the atoms of the $Zn^{2+}$–DBD complex. Two runs of MD 200 ps each were applied on the obtained structures to model the solvent state of the $Zn^{2+}$–DBD complex. In the first run, position restraint (the restraining force was $10,000\,kJ\,mol^{-1}\,nm^{-2}$) was applied on atoms of the $Zn^{2+}$–DBD complex. Then, the restraining force was decreased to $5000\,kJ\,mol^{-1}\,nm^{-2}$. Finally, 1 ns of MD simulation with no position restraints was applied to each of the resultant energy minimized structures of the solute complexes with the use of Berendsen temperature and pressure coupling (Berendsen, Postma, van Gunsteren, & Haak, 1984). In all the cases, bond length was constrained using the A linear constraint solver for molecular simulations algorithm (Hess, Bekker, Berendsen, & Fraaije, 1997).

### Statistical analysis of MD trajectories

Statistical analysis was performed for the MD trajectories of the obtained structures of the G245C, G245D, and WT p53 DBD that included: two $Zn^{2+}$-free mutant p53 DBD forms, two mutant p53 DBD complexes with $Zn^{2+}$ bound to the normal site, two mutant p53 DBD complexes with $Zn^{2+}$ bound to the found potential sites, and two WT p53 DBD structures, one $Zn^{2+}$-free, other $Zn^{2+}$-bound. As a result, eight starting structures were prepared. For each of them, 12 independent MD simulations were performed as described in the preceding section. The distribution of the starting velocities of particles in each simulation differed from the distributions in the other 11 simulations.

For each MD trajectory, the $Zn^{2+}$–DBD complexes corresponding to the last 30 ps of MD were retrieved. As a result, eight data-sets containing 30 time points each were generated. Each time point was represented by a single tertiary structure of WT or one of the mutant p53 DBD forms. Of these samples, two represented WT (one the $Zn^{2+}$-bound WT p53 and the other the $Zn^{2+}$-free WT p53). The other six samples represented the mutant p53 forms: the complexes of mutant p53 with $Zn^{2+}$ bound in the potential and in the normal sites and the $Zn^{2+}$-free mutant p53 forms.

To each sample, which represented either the $Zn^{2+}$–mutant p53 complex bound in a particular site or the $Zn^2$$^+$-free mutant p53, the Z-statistics was applied to determine deviations of the backbone atoms. For each p53 WT backbone atom represented by 12 points in space, the averaged value for each of the three Cartesian coordinates, i.e. for the centers of mass of a sample containing 12 points, was calculated. Then, the distance from each of the 12 points to the center of mass ($r_i$) was calculated. The obtained 12 distance values formed a sample of deviations from the average value for the position of a given atom at a given MD time point. For these 12 distances, the averaged value $\tilde{r}$ and standard deviation, $S_n$, were calculated:

$$\tilde{r} = \frac{1}{12} \sum_{i=1}^{12} r_i \tag{1}$$

$$S_n = \sqrt{\frac{1}{12} \sum_{i=1}^{12} (r_i - \tilde{r})^2} \tag{2}$$

For each of these 12 points representing the same WT backbone atom, the distance to the WT center of mass defined earlier was calculated. This value was used to calculate the Z-statistics value:

$$Z_i = \frac{r_0 - \tilde{r}}{S_n} \tag{3}$$

For the obtained $Z_i$ values, the arithmetic average was calculated so as to obtain the average Z-statistics for deviation of each mutant p53 DBD backbone atom from WT at a given MD time point:

$$Z^{(t)} = \frac{1}{12} \sum_{i=1}^{12} Z^{(t)} \tag{4}$$

Then, the yielded Z-statistics averages were averaged again over the MD time points, i.e. over 30 values corresponding to the last 30 ps of MD. Finally, the Z-statistics average was obtained for each atom of the backbone of the mutant p53 DBD:

$$\tilde{Z} = \frac{1}{30} \sum_{i=1}^{30} Z^{(t)} \tag{5}$$

## Results

### Search for $Zn^{2+}$-binding sites in tertiary structures of the p53 protein

Two potential $Zn^{2+}$-binding sites were found in the predicted mutant p53 structures that corresponded to the G245C and G245D substitutions. A new position of the bound $Zn^{2+}$ in the potential site of each of the mutant p53 forms was predicted with PDBSiteScan. These sites comprised residue positions 176, 242, and 245. Position 245 is not a part of the normal $Zn^{2+}$-binding site in the WT p53 (see Table 1).

According to prediction, the found $Zn^{2+}$-binding sites reside in the normal $Zn^{2+}$-binding pocket (Figure 1). In case of the potential $Zn^{2+}$-binding site predicted for the G245D (Figure 1(A)) atom of zinc binds to the sulfur atoms of amino acid residues 242C and 176C and to the oxygen atom of the amino acid residue 245D. In the template, which was used to predict this site (see Table 1), the fourth atom involved in the formation of a tetrahedral structure was the oxygen of the water molecule. In the case of the potential $Zn^{2+}$-binding site pre-

Table 1.  Substitutions in the p53 protein causing the appearance of the potential sites.

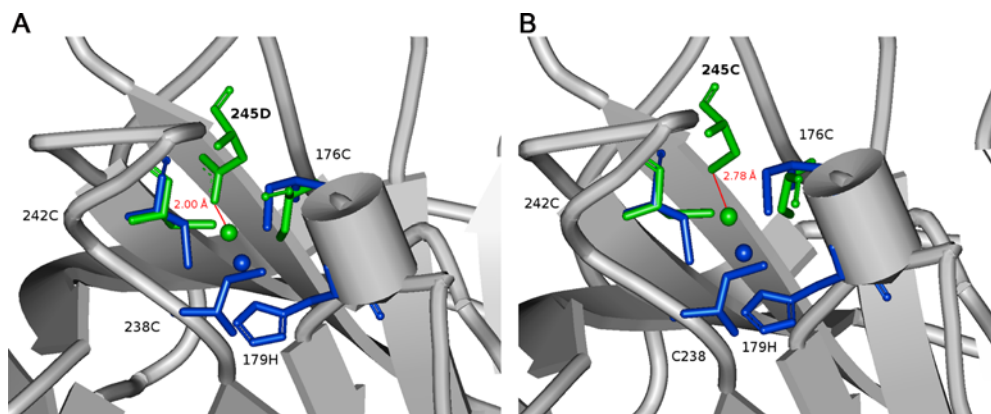| Substitution | PDBSITE ID | Template amino acid sequence | Template PDB ID |
|---|---|---|---|
| G245D | 1W5 MBC4 | 242C **245D** 176C | 1W5M |
| G245C | 1E51ZN | 242C **245C** 176C | 1E51 |
| WT | 1GZHZN1 | 176C 179H 238C 242C | 1GZH |



Figure 1.  Position of the normal $Zn^{2+}$-binding site and potential $Zn^{2+}$-binding site predicted for the G245D (A), G245C (B) mutants. The residues of the potential $Zn^{2+}$-binding sites of the mutant p53 forms are colored in green and those of the normal p53 $Zn^{2+}$-binding site are in blue. The $Zn^{2+}$ positions in the normal (blue) and potential (green) sites are shown as spheres.

dicted for the G245C (Figure 1(B)), zinc atom forms coordination bonds with the sulfur atoms of amino acid residues 242C, 245C, and 176C. The fourth atom involved in the formation of a tetrahedral complex can be the oxygen of the water molecule. The PDB structures of G245C/$Zn^{2+}$ and G245D/$Zn^{2+}$ complexes are provided as Supplementary data.

Previously, we suggested a possible mechanism for the impact of the function of the predicted potential sites on the activity of the mutant p53 forms. This mechanism is based on the presumable competition in $Zn^{2+}$ between a potential $Zn^{2+}$-binding site and a normal $Zn^{2+}$-binding site.

Thus, we predicted the appearance of a new $Zn^{2+}$-binding site resulting from mutations giving rise to the G245C and G245D substitutions in the p53 protein. It will be recalled that these substitutions are associated with the Li-Fraumeni syndrome and other cancers. The new site is located in close vicinity of the normal $Zn^{2+}$-binding site and it may compete with it in binding to $Zn^{2+}$, the allosteric regulator of p53 binding to DNA.

### *Analysis of conformational differences between the mutant and the WT p53 proteins*

Structural properties were monitored during the course of the trajectories to ascertain that the MD simulations were stable and converged. Structural changes were monitored by computing the root-mean-square deviation (RMSD) between snapshots obtained from MD trajecto-

ries and original starting coordinates. As an example, RMS deviations computed for several MD runs are shown in Figure 2. The figure shows that structures were stable with RMSD below 2.0 Å.
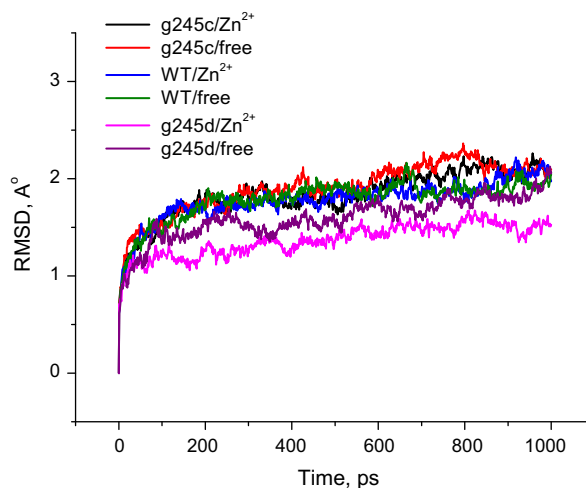


Figure 2.  Calculated RMS heavy atoms deviation (RMSD) of dynamic structures of different forms of p53 from initial structures vs. time from the MD simulation. Color of the lines corresponds to different forms of p53: black, the G245C mutant with $Zn^{2+}$ bound to the potential site; red, the Zn free G245C mutant; blue, the WT p53 in complex with $Zn^{2+}$ bound to the normal site; green, the Zn free WT p53; pink, the G245D mutant with $Zn^{2+}$ bound to the potential site; and purple, the Zn free G245D mutant.
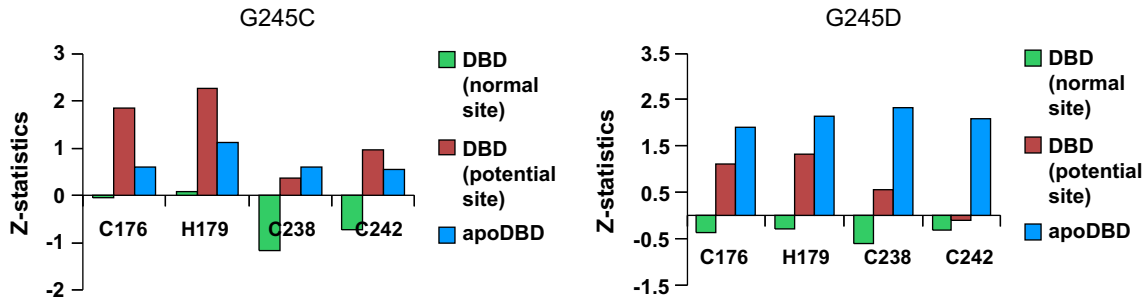
Figure 3.   The *Z*-statistics values for the residues of the $Zn^{2+}$-binding site in the G245C and G245D mutants.
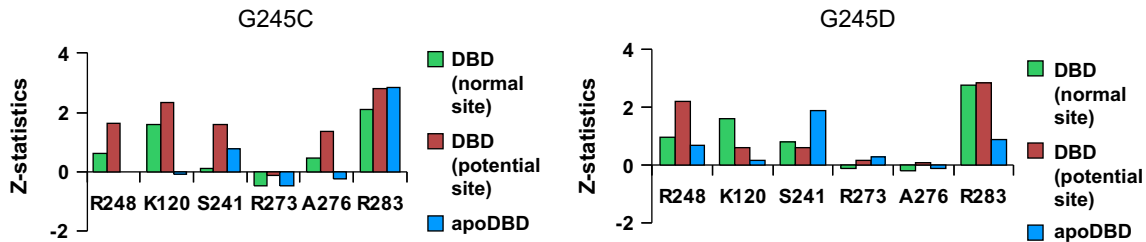


Figure 4.   The *Z*-statistics values for the residues of the DNA-binding site in the G245C and G245D mutants.

From inspection of the *Z*-statistics profiles for the MD trajectories, it is apparent that both G245C and G245D mutations in the $Zn^{2+}$-binding pocket have a strong impact on the conformation of the $Zn^{2+}$-binding site in the $Zn^{2+}$-free DBD, the impact of G245D being stronger.

Interestingly, when $Zn^{2+}$ was bound to the normal site, its conformation did not virtually differ from that of the WT p53 DBD. This meant that $Zn^{2+}$ stabilized its binding site. $Zn^{2+}$ binding in the potential sites of the p53 mutants gave rise to changes in the normal site conformation, with the effect being less pronounced for the G245D substitution (Figure 3).

Analysis of the conformational changes in the normal site is of interest because they may possibly lead to allosteric effects on the conformation of the DNA-binding protein regions.

$Zn^{2+}$ binding partially compensated substitution effect on the conformation of some regions of the DNA-binding motif; in contrast, the effect of the substitutions on the conformation of the DNA-binding site in the $Zn^{2+}$-unbound mutant p53 DBD was quite appreciable (Figure 4).

The conformations of the $Zn^{2+}$-free G245C and G245D differed most in the regions of the loop-sheet-helix (LSH) motif that binds the major DNA groove and of the structural loop that binds the minor DNA groove (Figure 5).

Comparisons of the *Z*-statistics profiles for the deviation of the backbone atoms of the two mutants from WT demonstrated that both had an influence on the conformation of the DNA-binding motif. However, G245C, unlike G245D, exerted no appreciable influence on the conformation of the LSH α-helix involved in DNA binding. Conversely, the L3 loop that made contact with the minor groove was subject to the influence of precisely G245C (Figure 6).

Thus, the *Z*-statistics profiles suggested that the conformational flexibility of the $Zn^{2+}$-binding pocket had an allosteric effect on the DNA-binding site.

The conformations of the G245C and G245D mutants in which $Zn^{2+}$ was bound in the normal and potential sites, differed most from each other in the region of the L2 loop involved directly in $Zn^{2+}$ binding. This was consistent with the notion that $Zn^{2+}$ binding influences the conformation of the L2 loop (Figure 7).
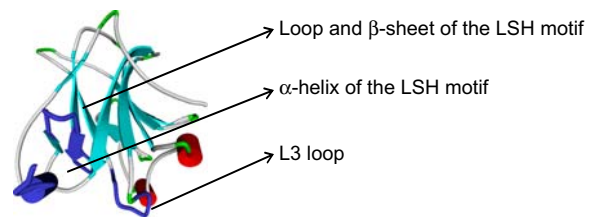


Figure 5.   The DNA-binding domain of the p53 protein. The structural elements of the DNA-binding site whose conformation is affected by the G245C and G245D mutations are highlighted in blue.
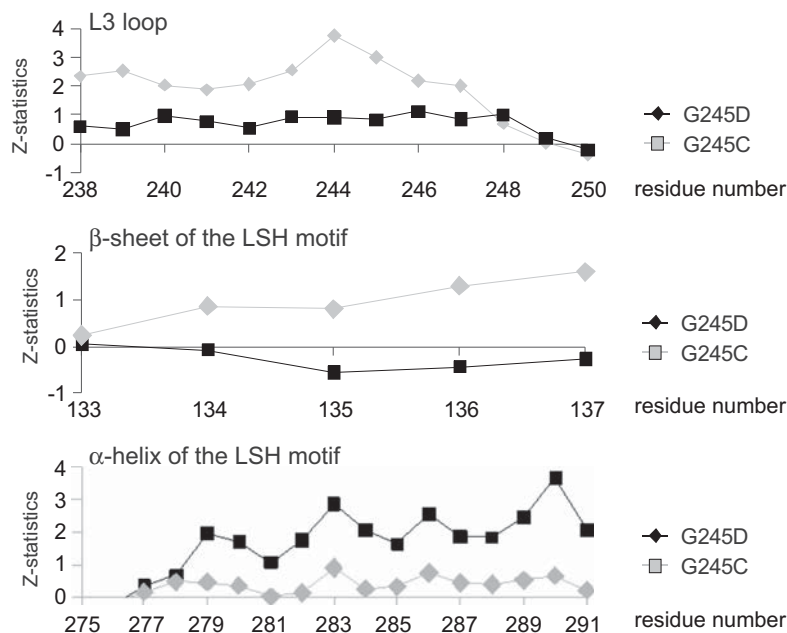
Figure 6.   The *Z*-statistics profiles for the structural elements of the $Zn^{2+}$-free p53 DBD whose conformation changed under effect of the G245C and G245D substitutions.

The *Z*-statistics profiles brought out the fact that the conformation of the L2 and L3 loops was less subjected to the effect of the two substitutions, when $Zn^{2+}$ was bound to the normal than to the potential $Zn^{2+}$-binding site. Interestingly, in case of $Zn^{2+}$ binding in the potential sites, the position of the R248 residue in the $Zn^{2+}$–DBD complexes, which made contact with the minor groove, was under the stronger influence of both mutations than in $Zn^{2+}$-free mutant forms of the p53 DBD. In contrast, $Zn^{2+}$ binding in the normal site in the G245C mutant form caused a smaller deviation of the R248 conformation from WT. This allowed us to infer that $Zn^{2+}$ binding to the potential sites produced a greater deviation of the DBD conformation from WT, as compared with $Zn^{2+}$ binding to the normal site.

Judging from the *Z*-statistics profiles, the G245C and G245D mutant forms differed markedly in their effect on DNA binding site conformation, depending on whether p53 was $Zn^{2+}$-free or $Zn^{2+}$-bound (Figure 7). As for the conformation of the L3 loop, it was not subjected appreciably to the influence of the G245D substitution, regardless of whether $Zn^{2+}$ was bound to the normal or potential site.

The reverse was observed for the G245C substitution. In case the $Zn^{2+}$ was bound to the potential site, it significantly changed the conformation of the DNA-bound L3 loop, as compared with the $Zn^{2+}$–WT DBD complex; in case of $Zn^{2+}$ binding to the normal site, the L3 loop conformation of the G245C mutant form was similar to the one characteristic of the $Zn^{2+}$–WT DBD complex.

Also, in case of $Zn^{2+}$ binding to the mutant p53 forms, the α-helix of the LSH motif, which made contacts with the major groove, was affected stronger by both substitutions irrespective of the $Zn^{2+}$ position (Figure 7). When $Zn^{2+}$ was bound to the normal site, the G245C substitution had the weakest effect on the conformation of the LSH α-helix, whose conformation was similar in all the four examined complexes, yet adopted different ones in the $Zn^{2+}$-free mutant forms.

## Discussion

The G245C and G245D substitutions influenced the $Zn^{2+}$-binding site conformation, on the one hand, and that of the p53 structural elements involved in DNA binding, on the other hand. This was evidence indicating that the conformation of the $Zn^{2+}$-binding site exerted an influence on that of the DNA-binding motif. A salient finding was that conformational changes in the $Zn^{2+}$-binding site affected not only the close R248 that made contact with the minor groove, but also the distant LSH motif involved in the binding of the major groove.

We have previously suggested that a new potential binding site that competes with the normal site in $Zn^{2+}$ binding may result from a hot-spot G245C substitution in the $Zn^{2+}$-binding pocket (Ivanisenko et al., 2005; Pintus et al., 2006, 2007). The current results support
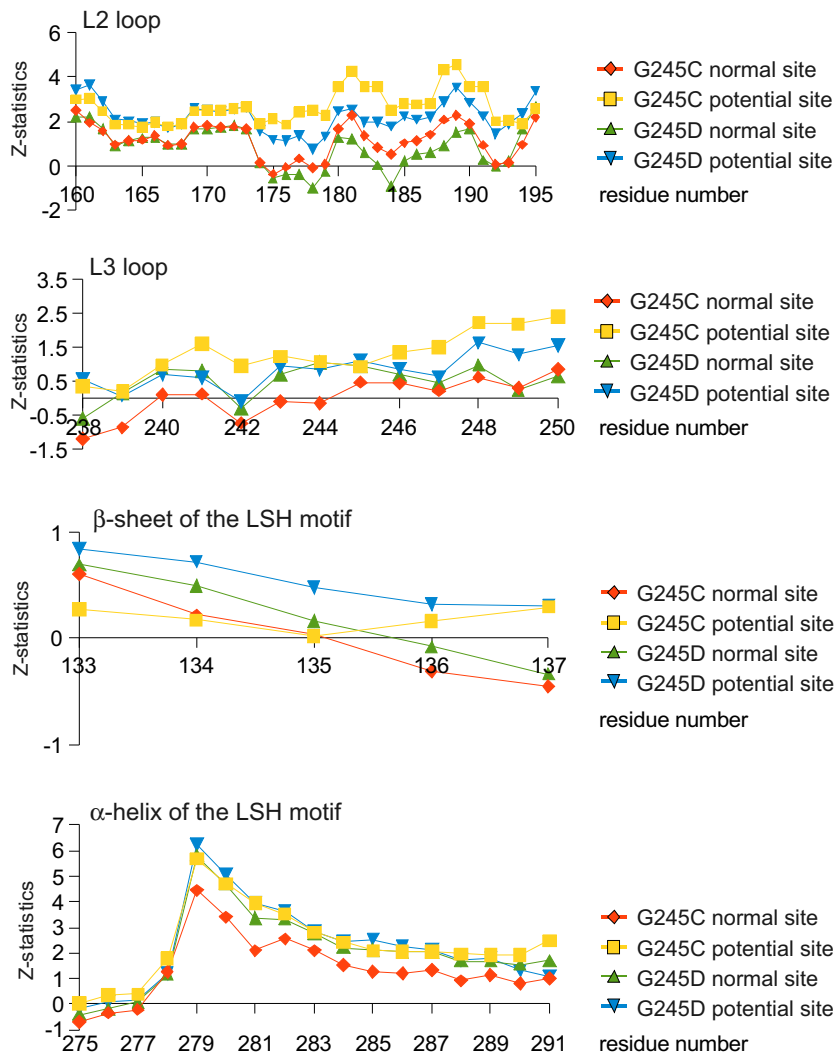
Figure 7.  The *Z*-statistics profiles for the $Zn^{2+}$-free structural elements of the p53 protein whose conformation changed under the effect of the G245C and G245D substitutions.

and extend our previous results by assuming that a potential $Zn^{2+}$-binding site may also be a consequence of another hot-spot G245D substitution. In the course of MD simulations of the mutant p53 forms, we obtained additional evidence that the shift of the $Zn^{2+}$ to the potential binding site resulted in conformational changes in both the $Zn^{2+}$-binding site and the DNA-binding motif.

We found that the influence of the substitutions in the $Zn^{2+}$-binding structural pocket spread not only to the DNA-binding L2 loop localized closely to the $Zn^{2+}$-binding site, but also to the LSH motif localized distantly from it. In this context, it is encouraging that in their earlier study (Duan & Nilsson, 2006) established a relation between closely localized structural elements of p53.

Recently, Khazanov and Levy (2011) have revealed that the α-helix of the LSH motif was important to non-

specific p53-DNA binding, while the L3 loop, by making a contact with the minor groove, provided specific p53-DNA binding. Reasoning further, it appeared plausible that the G245C and G245D substitutions, through their influence on the conformations of both the LSH motif and the L3 loop, have an impact on specific and nonspecific DNA-binding. When the effect of the G245C and G245D substitutions on nonspecific DNA-binding through the LSH motif was similar irrespective of the $Zn^{2+}$ position in DBD, their effect on specific DNA-binding through the L3 loop was dependent on the $Zn^{2+}$ position in the $Zn^{2+}$-binding site. In fact, the L3 loop conformation in the mutant forms of the p53 DBD differed from that of WT only when $Zn^{2+}$ occupied a potential site, but when it occupied the normal site, the L3 loop of the mutant form of the p53 DBD did not differ markedly from WT in conformation.

## Acknowledgments

## Supplementary material

The supplementary material for this paper is available online at http://dx.doi.org/10.1080/07391102.2012.691364.

## References

Alsner, J., Jensen, V., Kyndi, M., Offersen, B.V., Vu, P., Børresen-Dale, A.L., & Overgaard, J. (2008). A comparison between p53 accumulation determined by immunohistochemistry and TP53 mutations as prognostic variables in tumours from breast cancer patients. *Acta Oncologica, 47*, 600–607.

Amariglio, F., Tchang, F., Prioleau, M.N., Soussi, T., Cibert, C., & Méchali, M. (1997). A functional analysis of p53 during early development of *Xenopus laevis. Oncogene, 18*, 2191–2199.

Berendsen, H.J.C., Postma, J.P.M., van Gunsteren, W.F., & Haak, J.R. (1984). Molecular dynamics with coupling to an external bath. *Journal of Chemical Physics, 81*, 3684–3690.

Butler, J.S., & Loh, S.N. (2003). Structure, function, and aggregation of the zinc-free form of the p53 DNA binding domain. *Biochemistry, 42*, 2396–2403.

Coi, A., Tonelli, M., Ganadu, M.L., & Bianucci, A.M. (2006). Binding free energy calculations of adenosine deaminase inhibitors. *Bioorganic & Medicinal Chemistry, 14*, 2636–2641.

Donehower, L.A. (1997). Genetic instability in animal tumorigenesis models. *Cancer surveys, 29*, 329–352.

Duan, J., & Nilsson, L. (2006). Effect of $Zn^{2+}$ on DNA recognition and stability of the p53 DNA-binding domain. *Biochemistry, 45*, 7483–7492.

Esmann, U., Perera, L., Berkowitz, M.L., Darden, T., Lee, H., & Pedersen, L.G. (1995). A smooth particle mesh Ewald method. *Journal of Chemical Physics, 103*, 8577–8592.

Ewald, P.P. (1921). The calculation of optical and electrostatic lattice potentials. *Annalen der Physik, 64*, 253–287.

Hainaut, P., & Mann, K. (2001). Zinc binding and redox control of p53 structure and function. *Antioxidants & Redox Signaling, 3*, 611–623.

Hess, B., Bekker, H., Berendsen, H.J.C., & Fraaije, J.G.E.M. (1997). LINCS: A linear constraint solver for molecular simulations. *Journal of Computational Chemistry, 18*, 1463–1472.

Hess, B., Kutzner, C., van der Spoel, D., & Lindahl, E. (2008). GROMACS 4: Algorithms for highly efficient, load-balanced, and scalable molecular simulation. *Journal of Chemical Theory and Computation, 4*, 435–447.

Ivanisenko, V.A., Pintus, S.S., Grigorovich, D.A., & Kolchanov, N.A. (2004). PDBSiteScan: A program for searching for active, binding and posttranslational modification sites in the 3D structures of proteins. *Nucleic Acids Research, 32*, W549–W554.

Ivanisenko, V.A., Pintus, S.S., Grigorovich, D.A., & Kolchanov, N.A. (2005). PDBSite: A database of the 3D structure of protein functional sites. *Nucleic Acids Research, 33*, D183–D187.

Jorgensen, W., Chandrasekhar, J., Madura, J., Impey, R., & Klein, M. (1983). Comparison of simple potential functions for simulating liquid water. *Journal of Chemical Physics, 79*, 926–935.

Jorgensen, W., Maxwell, D., & Tirado-Rives, J. (1996). Development and testing of the OPLS all-atom force field on conformational energetics and properties of organic liquids. *Journal of American Chemical Society, 118*, 11225–11236.

Jorgensen, W., & Tirado-Rives, J. (1988). The OPLS [optimized potentials for liquid simulations] potential functions for proteins, energy minimizations for crystals of cyclic peptides and crambin. *Journal of American Chemical Society, 110*, 1657–1666.

Khazanov, N., & Levy, Y. (2011). Sliding of p53 along DNA can be modulated by its oligomeric state and by cross-talks between its constituent domains. *Journal of molecular biology, 408*, 335–355.

Levine, A.J. (1997). P53, the cellular gatekeeper for growth and division. *Cell, 88*, 323–331.

Lu, Q., Tan, Y.H., & Luo, R. (2007). Molecular dynamics simulations of p53 DNA-binding domain. *The Journal of Physical Chemistry B, 111*, 11538–11545.

Malkin, D., Li, F.P., Strong, L.C., Fraumeni, J.F. Jr, Nelson, C.E., Kim, D.H., … Tainsky, M.A. (1990). Germ line p53 mutations in a familial syndrome of breast cancer, sarcomas, and other neoplasms. *Science, 250*, 1233–1238.

Méplan, C., Richard, M.J., & Hainaut, P. (2000a). Metalloregulation of the tumor suppressor protein p53: Zinc mediates the renaturation of p53 after exposure to metal chelators *in vitro* and in intact cells. *Oncogene, 19*, 5227–5236.

Méplan, C., Richard, M.J., & Hainaut, P. (2000b). Redox signalling and transition metals in the control of the p53 pathway. *Biochemical Pharmacology, 59*, 25–33.

Merabet, A., Houlleberghs, H., Maclagan, K., Akanho, E., Bui, T.T., Pagano, B., … Nikolova, P.V. (2010). Mutants of the tumour suppressor p53 L1 loop as second-site suppressors for restoring DNA binding to oncogenic p53 mutations: Structural and biochemical insights. *Biochemical Journal, 427*, 225–236.

Olivier, M., Langerød, A., Carrieri, P., Bergh, J., Klaar, S., Eyfjord, J., … Børresen-Dale, A.L. (2006). The clinical value of somatic TP53 gene mutations in 1,794 patients with breast cancer. *Clinical Cancer Research, 12*, 1157–1167.

Pavletich, N.P., Chambers, K.A., & Pabo, C.O. (1993). The DNA-binding domain of p53 contains the four conserved regions and the major mutation hot spots. *Genes & Development, 7*, 2556–2564.

Pintus, S.S., Fomin, E.S., Ivanisenko, V.A., & Kolchanov, N.A. (2006). Phylogenetic analysis of the family of p53. *Biofizika, 51*, 640–649.

Pintus, S.S., Fomin, E.S., Oshurkov, I.S., & Ivanisenko, V.A. (2007). Phylogenetic analysis of the p53 and p63/p73 gene families. *In Silico Biology, 7*, 319–332.

Prochazkova, J., Lichnovsky, V., Kylarova, D., Erdosova, B., & Vranka, P. (2004). Involvement of p53 and Bcl-2 family proteins in regulating programmed cell death and proliferation in human embryogenesis. *General Physiology and Biophysics, 23*, 209–229.

Rainwater, R., Parks, D., Anderson, M.E., Tegtmeyer, P., & Mann, K. (1995). Role of cysteine residues in regulation of p53 function. *Molecular and Cellular Biology, 15*, 3892–3903.

Schwede, T., Kopp, J., Guex, N., & Peitsch, M.C. (2003). SWISS-MODEL: An automated protein homology-modeling server. *Nucleic Acids Research, 31*, 3381–3385.

van Slooten, H.J., van De Vijver, M.J., Borresen, A.L., Eyfjörd, J.E., Valgardsdóttir, R., Scherneck, S., … van Dierendonck, J.H. (1999). Mutations in exons 5-8 of the p53 gene, independent of their type and location, are associated with increased apoptosis and mitosis in invasive breast carcinoma. *The Journal of Pathology, 189*, 504–513.

Verhaegh, G.W., Parat, M.O., Richard, M.J., & Hainaut, P. (1998). Modulation of p53 protein conformation and DNA-binding activity by intracellular chelation of zinc. *Molecular Carcinogenesis, 21*, 205–214.